## POLITECNICO DI TORINO Repository ISTITUZIONALE

### Structured black-box parameterized macromodels of integrated passive components

Original

Structured black-box parameterized macromodels of integrated passive components / Zanco, A.; Bradde, T.; De Stefano, M.; Grivet-Talocia, S.; Hoehne, G.; Brenner, P.. - ELETTRONICO. - (2021), pp. 5-8. ((Intervento presentato al convegno 2021 IEEE MTT-S International Microwave Symposium, IMS 2021 tenutosi a Atlanta, GA, USA nel 5-25 June 2021 [10.1109/IMS19712.2021.9574912].

Availability: This version is available at: 11583/2947677 since: 2021-12-23T12:32:45Z

Publisher: Institute of Electrical and Electronics Engineers Inc.

Published DOI:10.1109/IMS19712.2021.9574912

Terms of use: openAccess

This article is made available under terms and conditions as specified in the corresponding bibliographic description in the repository

Publisher copyright IEEE postprint/Author's Accepted Manuscript

©2021 IEEE. Personal use of this material is permitted. Permission from IEEE must be obtained for all other uses, in any current or future media, including reprinting/republishing this material for advertising or promotional purposes, creating new collecting works, for resale or lists, or reuse of any copyrighted component of this work in other works.

(Article begins on next page)

# Structured black-box parameterized macromodels of integrated passive components

A. Zanco<sup>#1</sup>, T. Bradde<sup>#2</sup>, M. De Stefano<sup>#3</sup>, S. Grivet-Talocia<sup>#4</sup>, G. Hoehne<sup>\$1</sup>, P. Brenner<sup>\$2</sup>,

<sup>#</sup>Dept. Electronics and Telecommunications, Politecnico di Torino, Italy <sup>\$</sup>Infineon Technologies AG, Neubiberg, Germany

<sup>#1</sup>alessandro.zanco@polito.it,<sup>#2</sup>tommaso.bradde@polito.it,<sup>#3</sup>marco.destefano@polito.it, <sup>#4</sup>stefano.grivet@polito.it,<sup>\$1</sup>gregor.hoehne@infineon.com,<sup>\$2</sup>pietro.brenner@infineon.com

Abstract—A novel black-box model representation and identification process is introduced, specifically designed to extract layout-scalable behavioral macromodels of passive integrated devices from sampled frequency-domain responses. An automated choice of structured frequency-domain basis functions enables extremely accurate approximations for responses characterized by high dynamic ranges over extended frequency bands, overcoming the main limitations of standard approaches. Numerical results confirm that the proposed structured approach provides robust and reliable scalable models, with guaranteed stability and passivity over the frequency band and parameter space of interest.

*Keywords* — Passive device modeling, behavioral modeling, macromodeling, passivity, stability, parameterization.

#### I. INTRODUCTION

This paper aims at constructing behavioral macromodels [1] for integrated passive devices, such as multi-tap inductors or transformers. The reference application is circuit design for automotive radar IC's, although the methodology that is discussed is general and in principle applicable to any type of linear and passive multiport structure for various application fields.

The models we consider are scalable and embed in some parameterized closed form the dependence of the system response on several design parameters. Scalable (parameterized or multivariate) models provide extremely useful tools for designers, provided that

- their frequency responses accurately match reference data obtained from high-fidelity electromagnetic field solvers; the same level of accuracy should apply also to any derived Figure of Merit (FoM) of interest, such as single-ended, differential or common-mode resistances, inductances, and associated quality factors;
- they can be synthesized as compact SPICE-compatible behavioral netlists, to be employed in any type of analysis as provided by common circuit simulators, including frequency-domain (FD), time-domain (TD), harmonic balance (HB), sensitivity and Monte-Carlo sweeps.
- they are guaranteed stable and passive throughout the whole allowed parameter space.

Behavioral models having these features can be safely employed in design verification, optimization, centering, what-if and robustness/sensitivity analyses. The above requirements are extremely stringent and challenging for parameterized macromodels, as they imply:

- an accurate DC response, so that the operating point computed by circuit solvers in setting up system-level TD simulations is correct;
- a fine control of broadband accuracy throughout the frequency bands of interest. In particular, error control is very difficult to achieve in the entire parameter space for responses having a high dynamic range and possibly DC zeros;
- embedding stability and passivity constraints in the model training phase, where model coefficients are computed by a suitable fitting process.

This work builds on existing approaches for passive parameterized macromodeling, and suggests a modified model structure that significantly improves broadband accuracy of the models, still ensuring uniform stability, passivity, and compatibility with standard circuit solvers once exported to a behavioral SPICE model netlist.

#### II. PROPOSED MODEL STRUCTURE

Let us consider an integrated passive component with P electrical ports. A reference example that we will consider in this work is a coil with one or more center taps and a guard ring. The electrical ports i = 1, ..., P will include the inductor terminals i = 1, 2, the center taps i = 3, ..., P - 1 and the guard ring i = P, all referenced to a common ground through the substrate. The individual elements of the  $P \times P$  scattering matrix are characterized by a dominant inductive or capacitive behavior, leading to a large dynamic range over a frequency band starting from DC up to the frequency of interest. For the applications we consider in this work, the modeling frequency band is  $\Omega = [0, \omega_{\text{max}}]$  with  $\omega_{\text{max}} = 100$  GHz.

We aim at building scalable models, that represent in some closed parameterized form the dependence on a number  $\rho$  of independent parameters, collected in vector  $\vartheta = [\vartheta^1, \vartheta^2, ..., \vartheta^{\rho}]^T$ . For the integrated spiral inductor example these parameters may include trace width, separation, inner radius, substrate permittivity, etc. We will assume that the  $\rho$ -dimensional parameter space is a hyper-rectangle  $\Theta \subseteq \mathbb{R}^{\rho}$  defined as the Cartesian product of intervals  $[\vartheta^i_{\min}, \vartheta^i_{\max}]$ .

As opposed to physics-based models [2], where a fixed model topology is prescribed and component values are trained

based on multivariate fitting over frequency and parameter space, we proposed here a pure black-box model. Although this physics-based equivalent circuit modeling (ECM) is the standard in current circuit design practice, easy to interpret ECM's provide only limited accuracy in the higher frequency range; they may not be accurate enough for post-layout system verification, where field solver accuracy is required.

Black-box models are defined by a model structure and free coefficients, which are identified through a fitting process. The usual model structure spans the general class of multivariate rational functions. It is therefore expected that the model accuracy in both frequency domain and parameter space with respect to reference frequency responses can be set to an arbitrarily low and aggressive value, by properly choosing model orders.

The standard model structure we build on is the following barycentric form [3]–[5]

$$\mathbf{H}(s,\boldsymbol{\vartheta}) = \frac{\sum_{n=0}^{N} \mathbf{R}_{n}(\boldsymbol{\vartheta})\varphi_{n}(s)}{\sum_{n=0}^{N} r_{n}(\boldsymbol{\vartheta})\varphi_{n}(s)}$$
(1)

where  $\varphi_n(s) = \frac{1}{s-q_n}$  based on a set of *basis poles*  $q_n$  for n > 0 and  $\varphi_0(s) = 1$ . The coefficients  $\mathbf{R}_n(\boldsymbol{\vartheta})$  and  $r_n(\boldsymbol{\vartheta})$  of numerator and denominator are further expanded in the parameter space as [6], [7]

$$\mathbf{R}_{n}(\boldsymbol{\vartheta}) = \sum_{\ell} \mathbf{R}_{n,\ell} \xi_{\ell}(\boldsymbol{\vartheta}), \quad r_{n}(\boldsymbol{\vartheta}) = \sum_{\ell} r_{n,\ell} \xi_{\ell}(\boldsymbol{\vartheta}) \qquad (2)$$

where the basis functions  $\xi_{\ell}$  can be multivariate polynomials, trigonometric functions, radial basis functions, or any other choice that is appropriate. In this work, we use multivariate Chebychev polynomials. The model coefficients  $\mathbf{R}_{n,\ell}$  and  $r_{n,\ell}$  are identified through multivariate fitting based on a set of precomputed or adaptively computed frequency response samples  $\check{\mathbf{H}}(j\omega_k, \vartheta_m)$ , usually available through a full-wave (3D) or planar (2.5D) field solver. This process, which minimizes the model-data error

$$\sum_{k,m} \left\| \mathbf{H}(\mathbf{j}\omega_k, \boldsymbol{\vartheta}_m) - \breve{\mathbf{H}}(\mathbf{j}\omega_k, \boldsymbol{\vartheta}_m) \right\|^2$$
(3)

in some prescribed norm is standard, see e.g. [6]-[8].

The expansion (1) has been used and documented extensively by several Authors. However, it may fail to reproduce with good accuracy responses with high dynamic ranges, such as inductive or capacitive couplings characterized by low-frequency or DC zeros. In fact, a DC zero is not enforced in the standard model structure (1). Failing to enforce a DC zero on a response may lead to incorrect low-frequency behavior, which may result in unrealistic losses or spurious resistive couplings, wrong DC bias determination in system-level simulations, and other artefacts. A DC zero can be enforced in various ways, such as

• using a weighted error norm instead of (3), with a frequency-dependent weight  $w(\omega_k)$  that emphasizes the low-frequency band; this approach often deteriorates accuracy at high frequencies;

- minimize a relative error instead of the absolute error in (3); this implies using a frequency-dependent weight  $w(\omega_k)$  inversely proportional to the magnitude of each individual response; this approach has the same disadvantage of seriously deteriorating model accuracy at high frequencies;
- adding equality constraints in the fitting, so that the explicit DC model value H<sub>i,j</sub>(0, ϑ<sub>m</sub>) = 0 is enforced at machine precision; this approach has the disadvantage of bringing an unrealistically large number of constraints in a multivariate setting (each training point in the parameter space must be associated with an explicit constraint); in addition, this approach does not guarantee that the DC zero is present at arbitrary parameter values ϑ that do not belong to the training dataset, due to interpolation errors.

We resolve the above difficulties by embedding in the model structure the presence of DC zeros, only for those responses for which these zeros are expected. This is achieved by adopting the modified model structure

$$\mathbf{H}(s,\boldsymbol{\vartheta}) = \frac{\sum_{n=0}^{N} \mathbf{R}_{n}(\boldsymbol{\vartheta}) \circ \Phi_{n}(s)}{\sum_{n=0}^{N} r_{n}(\boldsymbol{\vartheta})\varphi_{n}(s)}$$
(4)

where  $\circ$  denotes the Hadamard product and

$$\Phi_n^{(i,j)}(s) = \begin{cases} \varphi_n(s) & \text{if } \quad \check{H}_{i,j}(s=0,\vartheta) \neq 0\\ \varphi_n^0(s) & \text{if } \quad \check{H}_{i,j}(s=0,\vartheta) = 0 \end{cases}$$
(5)

based on the modified (high-pass) basis function

$$\varphi_n^0(s) = \frac{s}{s - q_n}.$$
(6)

Model identification based on the structure (4) is compatible with consolidated fitting processes based on the Parameterized Sanathanan-Koerner iteration [6]–[8], which is not repeated here. The model poles  $p_n(\vartheta)$  are provided by the denominator zeros and are parameter-dependent. These poles can be constrained to be uniformly stable by adopting positive definite basis functions  $\xi_{\ell}(\vartheta)$  and enforcing the denominator coefficients to be non-negative via simple linear inequality constraints, see [9], [10]. Model passivity is checked through a modified multivariate Hamiltonian check inspired by [11], which provides localization of passivity violations. The latter are removed by a standard iterative perturbation. Finally, model synthesis to a parameterized SPICE netlist is obtained as in [9].

#### III. RESULTS

We apply the proposed macromodeling strategy to a parameterized 9-port integrated transformer, where both windings include 2 taps, and where an additional port is defined on the surrounding guard ring to model return path losses through the silicon substrate. The training data includes  $\bar{m} = 7$  frequency response matrices  $\mathbf{H}(j\omega_k, \vartheta_m)$  parameterized by the trace width of both coils conductors. Each individual response spans the bandwidth from DC to 100 GHz with K = 156 samples. Using these training data we build a parameterized model with  $\bar{n} = 4$  common poles

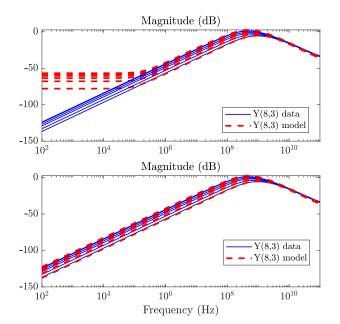


Fig. 1. Comparing model responses to reference data for a selected inter-winding coupling responses. Different curves correspond to different parameter (trace width) values. Top panel: standard model structure. Bottom panel: proposed model structure.

and degree  $\bar{\ell} = 1$  expansions (2) for both numerator and denominator in (4).

Figure 1 compares the results of the standard approach (top panel) based on the barycentric form (1) with the proposed model structure (4) (bottom panel). As opposed to the standard approach, the proposed model structure is able to recover the broadband dynamic range of the data with good accuracy, even at low frequencies. A correct representation is attained for the asymptotic low-frequency behavior of this response, which vanishes at DC. The standard approach, although overall accuracy is well below engineering practice (absolute error about  $10^{-3}$ ), provides unacceptable results, since the saturation to a finite DC level corresponds to a direct resistive path between first and second winding, which is physically inconsistent with the true behavior of the device.

The proposed structured macromodeling approach provides also improved accuracy for those Figures of Merit (FoMs) that are of interest for design purposes. We illustrate this point on another test case, a simple 3-port integrated inductor designed to operate in a single-ended configuration. The FoMs of interest are the frequency-dependent single-ended inductance  $L_{se}$  and the associated quality factor  $Q_{se}$ . A parameterized structured macromodel (4) was generated with  $\bar{n} = 10$  poles and  $\bar{\ell} = 2$  degree expansions with respect to conductor trace width, obtaining a model-data error (3) evaluated on a set of validation parameter samples of  $1.61 \cdot 10^{-2}$ .

We remark that any FoM is a derived quantity, which can be evaluated based on selected model responses in scattering or admittance forms [2]. Therefore, the accuracy in derived FoMs may be deteriorated due to sensitivity and error propagation in the application of the appropriate conversion formulas. It turns

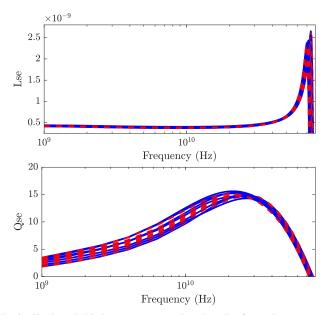


Fig. 2. Single-ended inductance (top panel) and quality factor (bottom panel) of a 3-port inductor, computed from proposed structured model (red dashed lines) and compared to reference data (blue solid lines). Different curves in the same panel denote different values of conductor width.

out that proposed approach is able to preserve accuracy in this conversion, due to the correct asymptotic behavior that is enforced. This is demonstrated in Figure 2, where we compare the FoMs computed on the training reference data to the FoMs derived from the model. We see that for both  $L_{se}$  and  $Q_{se}$  the model is able to recover the desired FoMs within acceptable error bounds. Thanks to the accurate black-box fitting, the accuracy on these metrics is much improved with respect to fixed-topology models such as [2], over the full bandwidth of interest.

#### REFERENCES

- S. Grivet-Talocia and B. Gustavsen, *Passive macromodeling: Theory and applications*. John Wiley & Sons, 2015, vol. 239.
- [2] V. Issakov, S. Kehl-Waas, and S. Breun, "Analytical equivalent circuit extraction procedure for broadband scalable modeling of three-port center-tapped symmetric on-chip inductors," *IEEE Transactions on Circuits and Systems I: Regular Papers*, vol. 66, no. 9, pp. 3557–3570, Sep. 2019.
- [3] D. Deschrijver, L. Knockaert, and T. Dhaene, "A barycentric vector fitting algorithm for efficient macromodeling of linear multiport systems," *IEEE Microwave and Wireless Components Letters*, vol. 23, no. 2, pp. 60–62, Feb 2013.
- [4] A. C. Antoulas and B. D. O. Anderson, "On the scalar rational interpolation problem," *IMA Journal of Mathematical Control and Information*, vol. 3, no. 2-3, pp. 61–88, 1986.
- [5] A. C. Antoulas, Approximation of large-scale dynamical systems. Society for Industrial and Applied Mathematics, 2005.
- [6] D. Deschrijver, T. Dhaene, and D. De Zutter, "Robust parametric macromodeling using multivariate orthonormal vector fitting," *IEEE Transactions on Microwave Theory and Techniques*, vol. 56, no. 7, pp. 1661–1667, July 2008.
- [7] P. Triverio, S. Grivet-Talocia, and M. S. Nakhla, "A parameterized macromodeling strategy with uniform stability test," *IEEE Trans. Advanced Packaging*, vol. 32, no. 1, pp. 205–215, Feb 2009.
- [8] C. Sanathanan and J. Koerner, "Transfer function synthesis as a ratio of two complex polynomials," *Automatic Control, IEEE Transactions on*, vol. 8, no. 1, pp. 56–58, jan 1963.

- [9] S. Grivet-Talocia and R. Trinchero, "Behavioral, parameterized, and broadband modeling of wired interconnects with internal discontinuities," *IEEE Transactions on Electromagnetic Compatibility*, vol. 60, no. 1, pp. 77–85, 2018.
  [10] A. Zanco, S. Grivet-Talocia, T. Bradde, and M. De Stefano,
- [10] A. Zanco, S. Grivet-Talocia, T. Bradde, and M. De Stefano, "Uniformly stable parameterized macromodeling through positive definite basis functions," *IEEE Transactions on Components, Packaging and Manufacturing Technology*, vol. 10, no. 11, pp. 1782–1794, Nov 2020.
- [11] A. Zanco, S. Grivet-Talocia, T. Bradde, and M. De Stefano, "Enforcing passivity of parameterized lti macromodels via hamiltonian-driven multivariate adaptive sampling," *IEEE Transactions on Computer-Aided Design of Integrated Circuits and Systems*, vol. 39, no. 1, pp. 225–238, 2018.